OXFORD Toxicology Research

Toxicology Research, 2025, **14**, 1–12
https://doi.org/10.1093/toxres/tfae225
Paper

Ginkgo biloba extract alleviates ferroptosis in lung epithelial cells induced by cigarette smoke extract through miR-3,619-5p/GPX4 axis

Anhui Xu[1,†], Yanmei Xu[1,†], Hongbo Chen[2,†], Linhua Xiang[1], Xiao Zhao[3,*]

[1]Department of Clinical Laboratory, The People's Hospital of Mengzi, No. 89 Tianma Road, Mengzi, Yunnan Province 661100, China,
[2]Department of Respiratory and Critical Care Medicine, Anning First People's Hospital Affiliated with Kunming University of Science and Technology, No. 2, Ganghe South Road, Anning, Yunnan Province 650302, China,
[3]Department of Respiratory and Critical Care Medicine, The People's Hospital of Mengzi, No. 89 Tianma Road, Mengzi, Yunnan Province 661100, China
*Corresponding author: Department of Respiratory and Critical Care Medicine, The People's Hospital of Mengzi, Yunnan Province 661100, China. No. 89 Tianma Road, Mengzi City. Email: 13466279233@163.com
[†]Anhui Xu, Yanmei Xu and Hongbo Chen contributed equally to this study.

Ginkgo biloba extract (GBE), a therapeutic drug, has anti-inflammatory and antioxidant effects that protect cells from harmful substances. Although GBE has been extensively studied in the prevention and treatment of lung diseases, its mechanism of action in chronic obstructive pulmonary disease (COPD) is unclear. In the present study, cigarette smoke extract (CSE) and cigarette smoke (CS) were used to induce COPD in cell and animal models. The expression of related genes and proteins was detected, and cell damage and lung tissue damage were evaluated via CCK-8 assays, flow cytometry analyses, ELISA, and HE staining. In HBE cells, the expression of miR-3,619-5p was upregulated after CSE induction. However, GBE treatment alleviated the impact of CSE on HBE cell damage and alleviated COPD in vivo. In addition, GBE treatment increased the expression of GPX4 by inhibiting the expression of miR-3,619-5p, and it reduced the release of the IL-6, IL-8, and TNF-α inflammatory factors. Moreover, GBE treatment decreased the production of ROS and MDA, as well as decreased the expression of the ferroptosis-related protein ACSL4, and it promoted the production of GSH and the expression of FTH1. Further, GBE treatment improved cell viability, inhibited ferroptosis, and ultimately alleviated COPD. The present findings suggest that GBE alleviates the progression of COPD through the inhibitory effect of the miR-3,619-5p/GPX4 axis on the ferroptosis process and that GBE may be an effective treatment option for COPD.

Keywords: chronic obstructive pulmonary disease; *Ginkgo biloba* extract; miR-3,619-5p; GPX4; ferroptosis.

1 Introduction

Chronic obstructive pulmonary disease (COPD) is a preventable and treatable disease characterized by airflow restriction, which is not fully reversible but develops progressively. COPD is associated with abnormal inflammatory responses and oxidative stress in the lungs in response to harmful gases or harmful particles, such as cigarette smoke (CS).[1] COPD is one of the most important causes of death in the world population, and smoking is an important cause of COPD.[2] Long-term stimulation of airway epithelial cells by CS can lead to the accumulation of reactive oxygen species (ROS), plasma membrane damage, inflammation, and eventually cell death.[3,4] Given the dangers of COPD, it is critical to discover new, targeted treatment strategies for this disease.

G. biloba is a traditional Chinese medicine in China. The Compendium of Materia Medica indicates that it has the effect of "calming asthma and relieving cough". Studies have shown that *ginkgo biloba* extract (GBE) has anti-inflammatory and antioxidant properties,[5,6] as well as preventive and therapeutic effects on cigarette smoke extract (CSE)-induced apoptosis in human pulmonary artery endothelial cells,[7] asthma,[8] pulmonary fibrosis,[9] and acute lung injury.[10] However, the mechanism of action of GBE in COPD is not fully understood. The present study explored the mechanism of GBE in preventing and treating the progression of COPD.

Ferroptosis is a complex iron-dependent cell death process involving intracellular iron accumulation, glutathione depletion, ROS formation, and lipid peroxide accumulation.[11] GPX4 is a negative regulator of ferroptosis and acts by regulating the process of lipid hydrogen peroxidation.[12,13] GPX4 also prevents lipid peroxidation caused by iron accumulation and effectively inhibits cell membrane damage.[14] Studies have shown that GPX4 deficiency in mice causes ferroptosis in renal tubular cells, leading to acute renal failure. Specific ferroptosis inhibitors (Fer-1) effectively prevent ferroptosis in renal tubular cells.[12] Ferroptosis is also associated with various lung diseases, including COPD, lung cancer, pulmonary fibrosis, and acute lung injury.[15] Similarly, CS-induced epithelial cell ferroptosis may be involved in the pathogenesis of COPD.[16] These studies suggest that ferroptosis plays an important role in the progression of COPD. In addition, studies have shown that GBE relieves airway inflammation in mice with COPD.[17] Moreover, GBE can promote the expression of ferroptosis markers GPX4

Received on 15 May 2024; revised on 31 October 2024; accepted on 17 December 2024

and FTH1, thereby protecting the kidney from ferroptosis and oxidative stress damage.[18] However, it remains unclear whether GBE alleviates COPD progression by affecting cellular ferroptosis.

Many microRNAs (miRNAs) are involved in the process of regulating ferroptosis.[19,20] Abnormal miRNA expression is a feature of many human diseases, and miRNAs play an active or negative role in disease development and progression.[21] miRNAs act on the 3′-untranslated region (3′-UTR) of mRNAs, regulate the stability and translation of the mRNA encoding the target protein, and negatively regulate gene expression at the posttranscriptional level.[22] In recent years, significant changes in multiple miRNAs have been reported in COPD, indicating that miRNAs directly or indirectly affect COPD.[23] In lung diseases, miR-3,619-5p inhibits the growth of non-small cell lung cancer (NSCLC) cells by reducing the expression of β-catenin.[24] The overexpression of miR-3,619-5p also inhibits the progression of NSCLC by inhibiting the expression of SALL4.[25] However, the regulatory mechanism of miR-3,619-5p in COPD has not been reported. Understanding the mechanism by which miR-3,619-5p regulates the progression of COPD will help develop new diagnostic and therapeutic strategies.

Based on the above analysis, we hypothesize that GBE may regulate ferroptosis through the miR-3,619-5p/GPX4 molecular axis, thereby alleviating the progression of COPD. To test this hypothesis, we conducted in vivo and in vitro studies using animal and cellular models of COPD. The present results will help to elucidate the process of COPD occurrence and provide new ideas and methods for the treatment of COPD.

2 Materials and methods

2.1 Cigarette smoke (CS)-induced animal model

Thirty male C57BL/6 mice (weighing 18–20 g) aged 6–8 weeks were obtained from the Animal Experimental Center. After one week of adaptive feeding, the experimental animals were randomly divided into three groups, with 10 mice in each group. A custom smoking room (70 cm × 50 cm × 40 cm) was designed to establish a CS exposure model. The mice were placed in a smoking room and exposed to CS throughout their body, as previously described.[26] In brief, the mice were exposed to the CS three times a day with six cigarettes (each cigarette containing 0.8 mg of nicotine and 10 mg of tar; Shishi, China) for a total of 12 weeks. The control group was exposed to filtered air. The GBE treatment group included Shuxuening injection (National Medicine Approval Number Z13020795, Hebei Shenwei Pharmaceutical Group Co., Ltd), with a concentration of 5 mL/tube, containing 17.5 mg of GBE, 4.2 mg of total flavonol glycosides, and 0.7 mg of ginkgolides. Starting from the sixth week, the medication was administered at a dosage of 0.4 mL/kg via intraperitoneal injection (once a day), whereas the control group received an intraperitoneal injection of physiological saline (once a day). Six weeks after administration, the mice were euthanized. The right lung was lavaged by ligation of the left main bronchus, and the alveolar lavage fluid was collected by repeated flushing with 0.3 mL of PBS three times. The left lung tissue was sectioned, processed, and extracted for the preparation of relevant proteins.

2.2 Preparation of cigarette extract (CSE)

CSE was extracted according to the method of FUJII et al.[27] In brief, 40 mL of cigarette smoke was inhaled into a syringe and slowly bubbled into sterile serum-free cell medium in a 15 mL BD Falcon tube. One cigarette was used to prepare 10 mL of solution. The CSE solution was filtered (0.22 μm) to remove insoluble particles and designated as 100% CSE solution.

2.3 Cell culture and transfection

The human bronchial epithelial (HBE) cell line was obtained from Shenzhen Haodi Otwo Biotechnology Co., Ltd, and it was cultured in DMEM (HyClone, USA), containing 10% fetal bovine serum and 1% penicillin streptomycin and streptomycin, and placed in an incubator for routine culture at 37 °C and 5% CO_2. First, cultured HBE cells were treated with 1%, 3%, or 5% CSE for 72 h to determine the effect of CSE on HBE cell damage. For subsequent experiments, HBE cells were pretreated with GBE for 1 h and then treated with 3% CSE for 72 h. For the erastin (ferroptosis activator) group, 5 μmol/L erastin was added.

HBE cells were incubated overnight in a 24-well plate, and when the cell density reached approximately 60–70%, the miR-3,619-5p mimic or miR-3,619-5p inhibitor was transfected into HBE cells according to the instructions of the Lipofectamine 3,000 reagent (Invitrogen, Carlsbad, CA, USA). The cells were cultured at 37 °C in a 5% CO_2 incubator for 48 h, and the transfection efficiency was detected.

2.4 CCK-8 detection of cell viability

The cells in the 96-well plates were precultured for 24 h according to the requirements of the different groups, and 10 μL of CCK-8 reagent (C0037, Beyotime, China) was then added to each well. The absorbance value at 450 nm was measured with a microplate reader.

2.5 Flow cytometry

HBE cells were collected, washed twice with PBS, and resuspended in 200 μL of PBS. The apoptosis rate was detected via an Annexin V-FITC/PI apoptosis assay kit (Absin, China).

2.6 ELISA detection of inflammatory factors

In accordance with the instructions for the TNF-α (SEKH-0047 or SEKM-0034, Solarbio, Beijing, China), IL-6 (SEKH-0013 or SEKM-0007, Solarbio), and IL-8 (SEKH-0016 or SEKM-0046, Solarbio) kits, HBE cell culture medium was transferred to a sterile centrifuge tube and centrifuged at 1000 × g at 4 °C for 10 min. The supernatant was then equally divided into small EP tubes for testing. The shredded mouse lung tissue was added to the corresponding volume of PBS (with a weight to volume ratio of 1:9) in a glass homogenizer and ground thoroughly on ice. To further lyse histiocytes, the homogenate was repeatedly frozen, thawed, and disrupted by ultrasound. Finally, the homogenate was centrifuged at 4 °C and 5,000 × g for 10 min, and the supernatant was collected for detection. After each working solution was added according to the instructions, the levels of cytokines (TNF-α, IL-6, and IL-8) were measured at an optical density of 450 nm via a microplate reader.

2.7 Reagent kits for detecting MDA, GSH, and Fe^{2+}

In accordance with the instructions of the cell MDA assay kit (A003–4-1, Jiancheng Bioengineering Institute, Nanjing, China), GSH kit (BC1175, Solarbio), and Fe^{2+} kit (ab83366, Abcam, UK), HBE cells were collected into a centrifuge tube. After centrifugation, the supernatant was discarded, and the cells were disrupted by ultrasonic waves. After centrifugation at 8000 × g and 4 °C for 10 min, the supernatant was removed and placed on ice for measurement. The contents of MDA, GSH, and Fe^{2+} in the cells were detected after the working solution was added to the supernatant.

Table 1. Primer sequences.

Target	Sequence (F: Forward prime; R: Reversed prime) (5 "-3")
miR-3,619-5p	F: CGTCAGCAGGCAGGCTGG
	R: AGTGCAGGGTCCGAGGTATT
U6	F: CTCGCTTCGGCAGCACA
	R: AACGCTTCACGAATTTGCG

2.8 ROS detection

HBE cells were incubated with a DCFH-DA probe (Sigma–Aldrich, USA) for 30 min at 37 °C. After removal of the supernatant, the cells were washed twice with DMEM without FBS. The images were observed under a fluorescence microscope.

2.9 Western blot detection

Proteins were extracted from HBE cells and lung tissues via RIPA buffer (Sigma–Aldrich, USA), separated via SDS–PAGE, and transferred to PVDF membranes (Millipore, USA). and the membranes were incubated with 5% skim milk for 1.5 h at room temperature and then incubated overnight at 4 °C with the following diluted primary antibodies (all were purchased from Abcam and diluted according to the manufacturer's instructions): Cytoc (ab133504), cleaved-caspase 3 (ab184787), cleaved-PARP (ab32064), GPX4 (ab125066), FTH1 (ab75973), ACSL4 (ab155282), and β-actin (ab8226). The membranes were then incubated with a secondary antibody (1:4000, ab97051, Abcam, UK) at room temperature for 1 h, and protein bands were observed with an enhanced chemiluminescence (ECL) kit (Millipore, USA). Finally, ImageJ software was used to conduct semiquantitative analysis of the bands.

2.10 RT-qPCR

Total RNA was extracted from HBE cells with TRIzol reagent, and cDNA was subsequently synthesized via reverse transcription. cDNA was used as a template for SYBR Green real-time fluorescence quantitative analysis. U6 was used as the internal reference gene, and the results were obtained via the $2^{-\Delta\Delta Ct}$ method. The detailed information of the primer sequences is shown in Table 1.

2.11 Dual-luciferase reporter gene assay

Biological information (https://www.targetscan.org/vert_80/) was used to predict the binding sites of miR-3,619-5p and GPX4. 3'-UTR wild-type GPX4 vectors (GPX4 WT) and mutant GPX4 vectors (GPX4 MUT) containing miR-3,619-5p binding sites were constructed. The vectors were cotransfected into 293 T cells with the miR-3,619-5p mimic or negative controls via Lipofectamine 3,000. After 48 h, the luciferase activity was detected via a dual luciferase reporting system.

2.12 RNA pull-down experiment

The sequence of miR-3,619-5p was synthesized in vitro (Gene Pharma, Shanghai, China). The Bio-miR-3,619-5p biotinylated probe was constructed with a biotinylated RNA labeling mixture, and the biotinylated probe and Pierce™ streptavidin agarose beads were mixed and cultured overnight at 4 °C. The cell lysates and RNase inhibitors were then added, followed by incubation on ice for 1 h. Protein detection was then performed via Western blot analysis.

2.13 HE staining

Mouse lung tissues were collected, made into paraffin sections, and dewaxed. The sections were stained with hematoxylin for 5 min, differentiated with 5% acetic acid for 1 min, treated with reverting blue solution for 1–2 min, and stained with eosin for 1 min. Finally, the sections were dehydrated in ethanol and sealed with neutral gum for observation and analysis.

2.14 TUNEL staining

The paraffin-embedded lung tissue sections were washed twice with PBS, and 50 μL of TUNEL detection solution (C1089, Beyotime, China) was added to the sections, followed by incubation at 37 °C in a dark wet box for 1 h. The sections were rinsed three times with PBS, sealed with glycerol, and observed under a fluorescence microscope, and images were acquired.

2.15 Statistical analysis

The data were analyzed via GraphPad Prism version 8 software (GraphPad, USA). All experiments were repeated at least 3 times. One-way ANOVA and t tests were used for statistical analysis. $p < 0.05$ was considered statistically significant.

3 Results

3.1 HBE cell damage is induced by CSE

The effect of CSE on HBE cells was evaluated using a CCK-8 assay to determine the cytotoxicity of CSE, which revealed that the viability of HBE cells decreased with increasing CSE concentration (Fig. 1A). Flow cytometry analysis revealed that the apoptosis rate of HBE cells increased with increasing CSE concentration (Fig. 1B). ELISA and oxidative stress assays revealed that the levels of IL-6, IL-8, TNF-α, MDA, and ROS increased with increasing CSE concentration (Fig. 1C–E); however, the GSH content decreased (Fig. 1F). Finally, Western blot analysis revealed that the expression levels of the Cytc, C-caspase3, and C-PARP apoptosis-related proteins increased with increasing CSE concentration, whereas the expression levels of the GPX4 and FTH1 ferroptosis-related proteins decreased with increasing CSE concentration. In addition, the level of ACSL4 increased with increasing CSE concentration (Fig. 1G). These results indicated that CSE induces HBE cell apoptosis and ferroptosis in a dose-dependent manner. In subsequent experiments, 3% CSE was selected to induce HBE cell damage.

3.2 GBE pretreatment alleviates HBE cell damage

The effects of GBE on CSE-induced HBE cell damage were subsequently analyzed. Cell viability increased with increasing GBE concentration (Fig. 2A), and a GBE concentration of 30 μg/mL was selected for subsequent experiments. The CCK-8 assay revealed that the addition of GBE significantly increased the viability of HBE cells compared with that in the CSE group (Fig. 2B). Flow cytometry analysis of cell apoptosis revealed that the addition of GBE inhibited HBE cell apoptosis (Fig. 2C). ELISA detection of inflammatory factors revealed that the addition of GBE significantly reduced the levels of IL-6, IL-8, and TNF-α compared with those in the CSE group (Fig. 2D). The oxidative stress assay revealed that the addition of GBE reduced the MDA and ROS levels (Fig. 2E and F) but increased the GSH levels (Fig. 2G). In addition, GBE inhibited the expression of the Cytc, C-caspase3 and C-PARP apoptosis-related proteins but promoted the expression of the GPX4 and FTH1 ferroptosis-related proteins, and inhibited the expression of ACSL4 (Fig. 2H). Therefore, these findings indicated

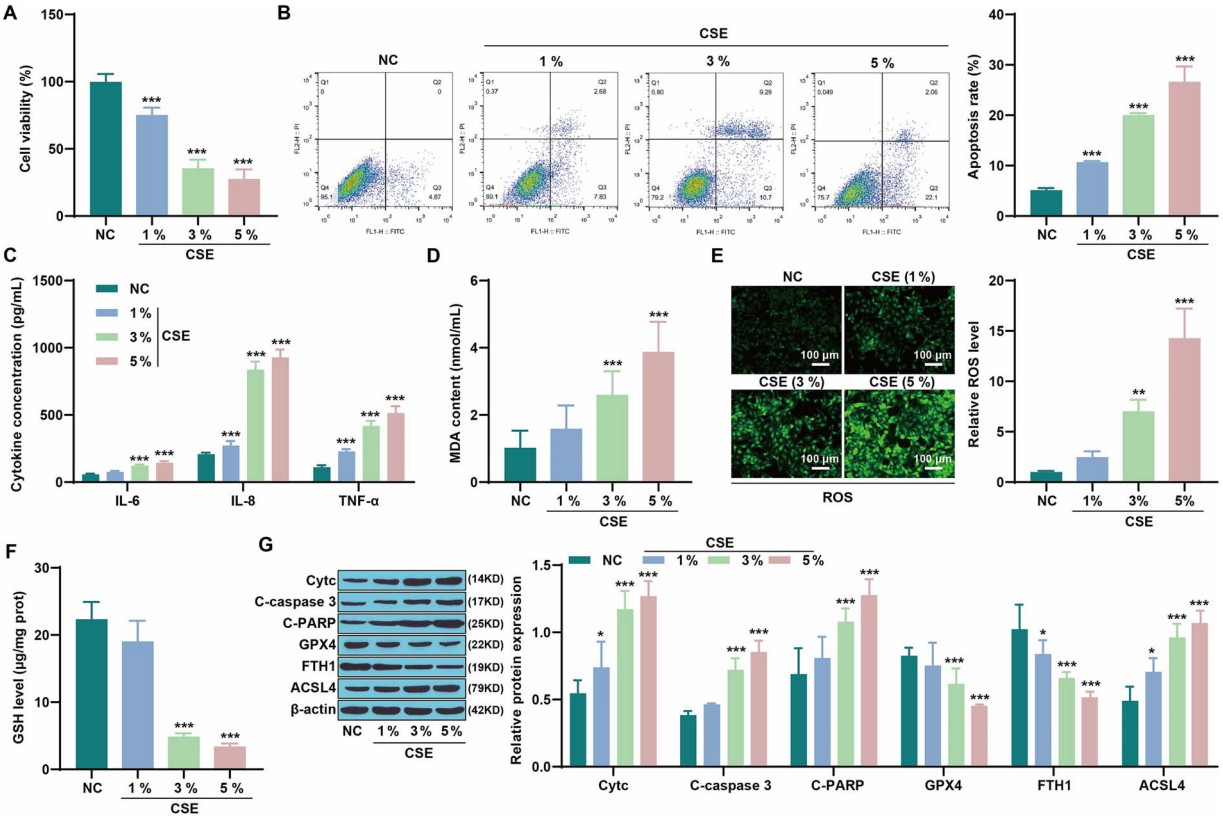

Fig. 1. CSE induces HBE cell damage. A: Cell viability was analyzed by a CCK-8 assay. B: Flow cytometry detection of cell apoptosis. C: ELISA detection of inflammatory factors. D-F: Oxidative stress levels were detected and analyzed via kits and a DCFH-DA fluorescent probe. G: Western blot analysis of the expression of related proteins. *P < 0.05, **P < 0.01 and ***P < 0.001 vs. NC.

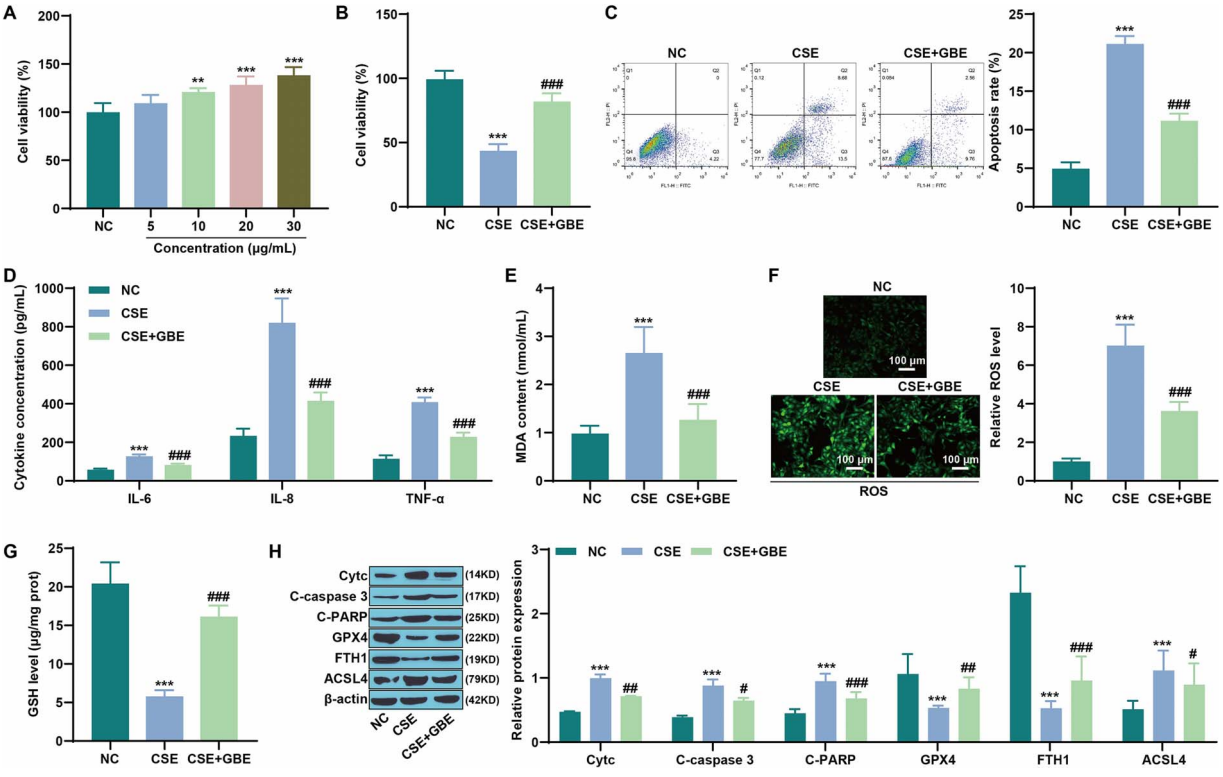

Fig. 2. GBE pretreatment alleviates CSE-induced HBE cell damage. A-B: Cell viability was analyzed by a CCK-8 assay. C: Flow cytometry detection of cell apoptosis. D: ELISA detection of inflammatory factors. E: Detection of MDA levels via a reagent kit. F: Detection of ROS levels via a DCFH-DA fluorescence probe. G: Detection of GSH levels via a reagent kit. H: Western blot analysis of the expression of related proteins. **P < 0.01, ***P < 0.001 vs. NC; #P < 0.05, ##P < 0.01, and ###P < 0.001 vs. CSE.

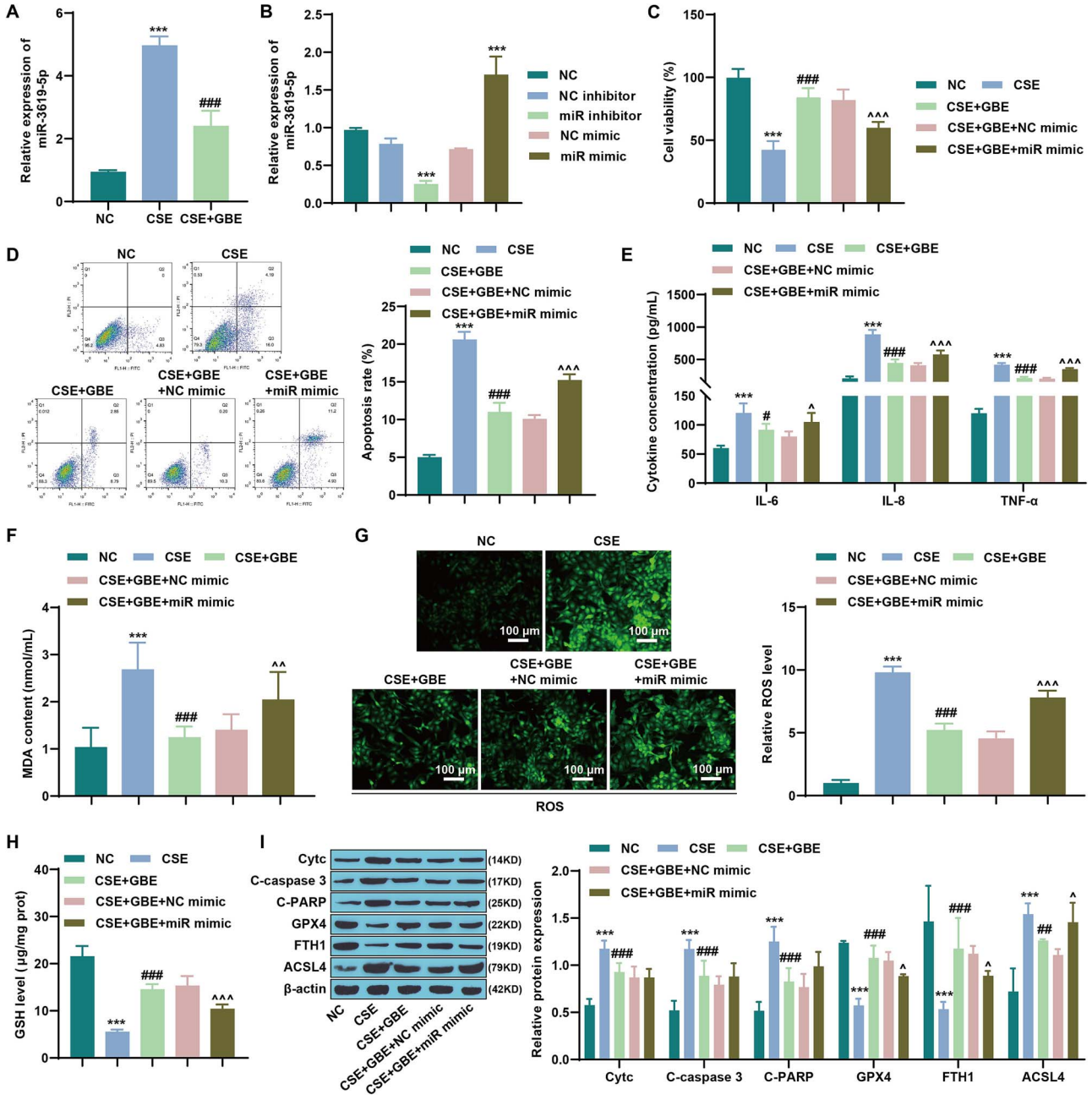

Fig. 3. miR-3,619-5p reverses the inhibitory effect of GBE on CSE-induced HBE cell damage. A: RT–qPCR detection of miR-3,619-5p expression. B: The transfection efficiency of miR-3,619-5p was detected via RT–qPCR. C: CCK–8 detection of cell viability. D: Flow cytometry detection of cell apoptosis. E: ELISA analysis of the levels of the IL-6, IL-8, and TNF-α inflammatory factors. F: Detection of MDA levels via a reagent kit. G: Detection of ROS levels via a DCFH–DA fluorescence probe. H: Detection of GSH levels via a reagent kit. I: Western blot analysis of protein expression. $^{***}P < 0.001$ vs. NC; $^{\#}P < 0.05$, $^{\#\#}P < 0.01$, and $^{\#\#\#}P < 0.001$ vs. CSE; $^{\wedge}P < 0.05$, $^{\wedge\wedge}P < 0.01$, and $^{\wedge\wedge\wedge}P < 0.001$ vs. CSE + GBE. miR mimic, miR-3,619-5p mimic; miR inhibitor, miR-3,619-5p inhibitor.

that GBE pretreatment has a protective effect on CSE-induced HBE cell damage, significantly reducing CSE-induced cell apoptosis and ferroptosis.

3.3 miR-3,619-5p reduces the protective effect of GBE against HBE cells

The above experiments demonstrated that GBE protected HBE cells from CSE-induced injury, but the downstream regulatory mechanism of GBE remained unknown. Because the regulatory role of miR-3,619-5p in lung diseases has been reported,[24,25] the present study explored the relationship between GBE and miR-3,619-5p in CSE-induced injury. Abnormally high expression of miR-3,619-5p was detected in CSE-treated HBE cells via RT–qPCR, and the expression level of miR-3,619-5p was suppressed by GBE (Fig. 3A). These findings indicated that GBE has a regulatory effect on the expression of miR-3,619-5p. The transfection efficiency of miR-3,619-5p was detected by RT–qPCR. The expression of miR-3,619-5p was significantly downregulated in the miR-3,619-5p inhibitor group and significantly upregulated in the miR-3,619-5p mimic group compared with the NC group (Fig. 3B), indicating successful transfection. Compared with the CSE + GBE group, the CCK-8 assay revealed that the viability of HBE cells

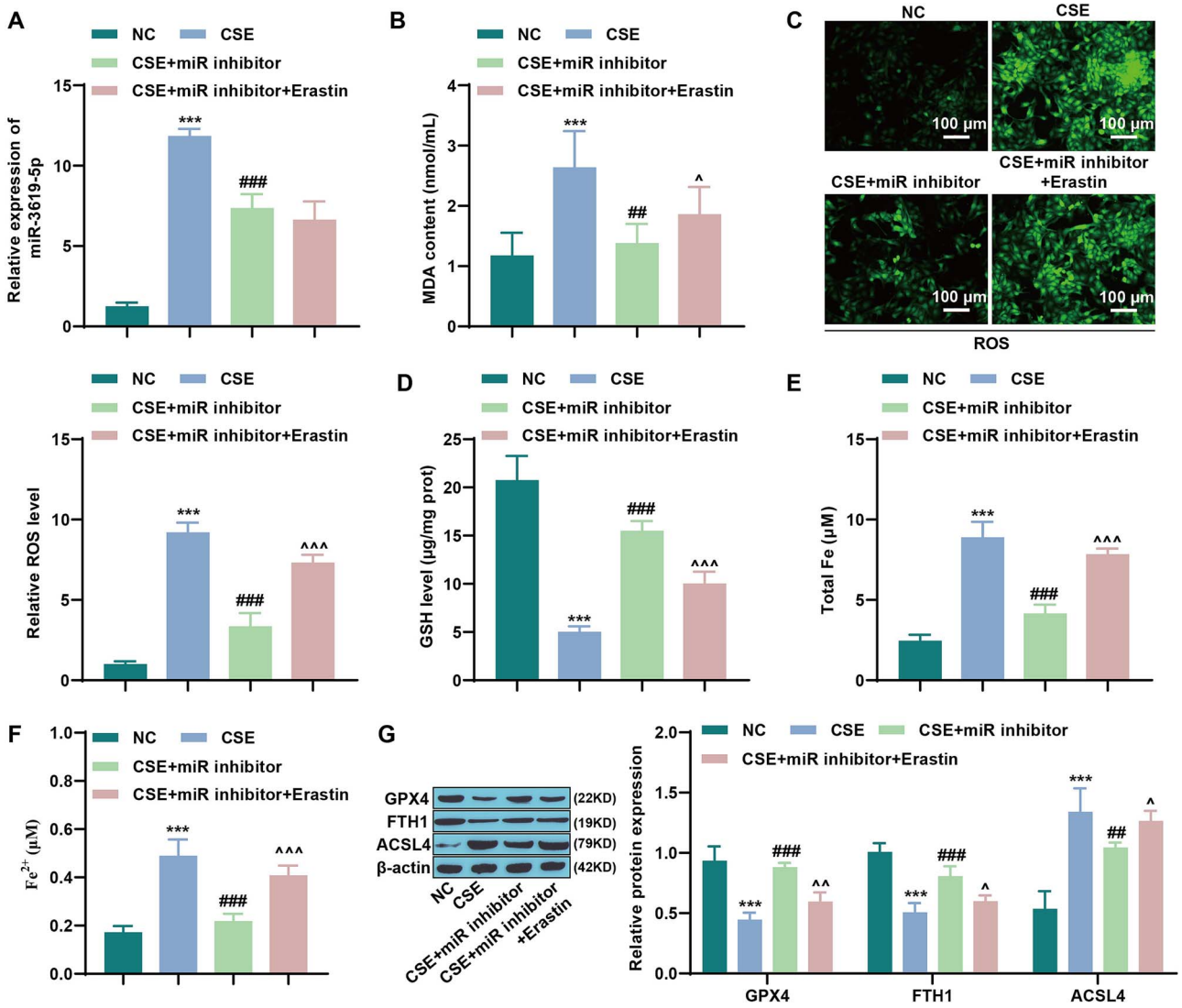

Fig. 4. miR-3,619-5p promotes CSE-induced ferroptosis in HBE cells. A: RT–qPCR detection of miR-3,619-5p expression. B: Detection of MDA levels via a reagent kit. C: Detection of ROS levels via a DCFH–DA fluorescence probe. D: Detection of GSH levels via a reagent kit. E: Detection of the total iron level via a reagent kit. F: Detection of Fe^{2+} levels via a reagent kit. G: Western blot analysis of ferroptosis-related proteins. $^{***}P < 0.001$ vs. NC; $^{\#\#}P < 0.01$ and $^{\#\#\#}P < 0.001$ vs. CSE; $^{\wedge}P < 0.05$, $^{\wedge\wedge}P < 0.01$, and $^{\wedge\wedge\wedge}P < 0.001$ vs. CSE + miR inhibitor. miR inhibitor, miR-3,619-5p inhibitor.

was lower in the miR-3,619-5p-overexpressing group (Fig. 3C), whereas the viability of HBE cells was greater in the miR-3,619-5p-knockdown group (Fig. S1A). Compared with the CSE + GBE group, miR-3,619-5p overexpression promoted HBE cell apoptosis (Fig. 3D), whereas miR-3,619-5p knockdown further inhibited HBE cell apoptosis (Fig. S1B). Compared with the CSE + GBE group, ELISA analysis revealed that miR-3,619-5p overexpression significantly increased the levels of IL-6, IL-8, and TNF-α (Fig. 3E) but that miR-3,619-5p knockdown further decreased the levels of IL-6, IL-8, and TNF-α (Fig. S1C). The oxidative stress assay revealed that miR-3,619-5p overexpression increased the MDA and ROS levels (Fig. 3F and G) but decreased the GSH levels (Fig. 3H), whereas miR-3,619-5p knockdown reduced the MDA and ROS levels (Fig. S1D and F) but increased the GSH levels (Fig. S1E). miR-3,619-5p overexpression did not significantly affect the expression of the Cytc, C-caspase3, and C-PARP apoptosis-related proteins. However, miR-3,619-5p overexpression inhibited the expression of GPX4 and FTH1, and it promoted the expression of ACSL4 (Fig. 3I). Moreover, miR-3,619-5p knockdown reversed the changes in the expression of ferroptosis-related proteins (Fig. S1G). These results indicated that GBE alleviates CSE-induced HBE cell damage by regulating miR-3,619-5p. miR-3,619-5p overexpression partially reverses the effect of GBE, but miR-3,619-5p affects only ferroptosis-related proteins and does not affect apoptosis-related proteins. Therefore, these findings indicated that GBE inhibits CSE-induced HBE cell ferroptosis through miR-3,619-5p.

3.4 miR-3,619-5p promotes CSE-induced ferroptosis in HBE cells

Because the above results demonstrated that miR-3,619-5p regulates the ferroptosis signaling pathway, the mechanism of this regulation was further investigated. Compared with the CSE group, detection of miR-3,619-5p expression demonstrated that the expression level of miR-3,619-5p was significantly downregulated after knockdown, while erastin (a ferroptosis activator) had no significant effect on the expression level of miR-3,619-5p (Fig. 4A). miR-3,619-5p knockdown inhibited the effect of CSE on the MDA and ROS levels but increased the GSH content. Moreover, erastin reversed the effect of miR-3,619-5p knockdown (Fig. 4B–D). In addition, miR-3,619-5p knockdown

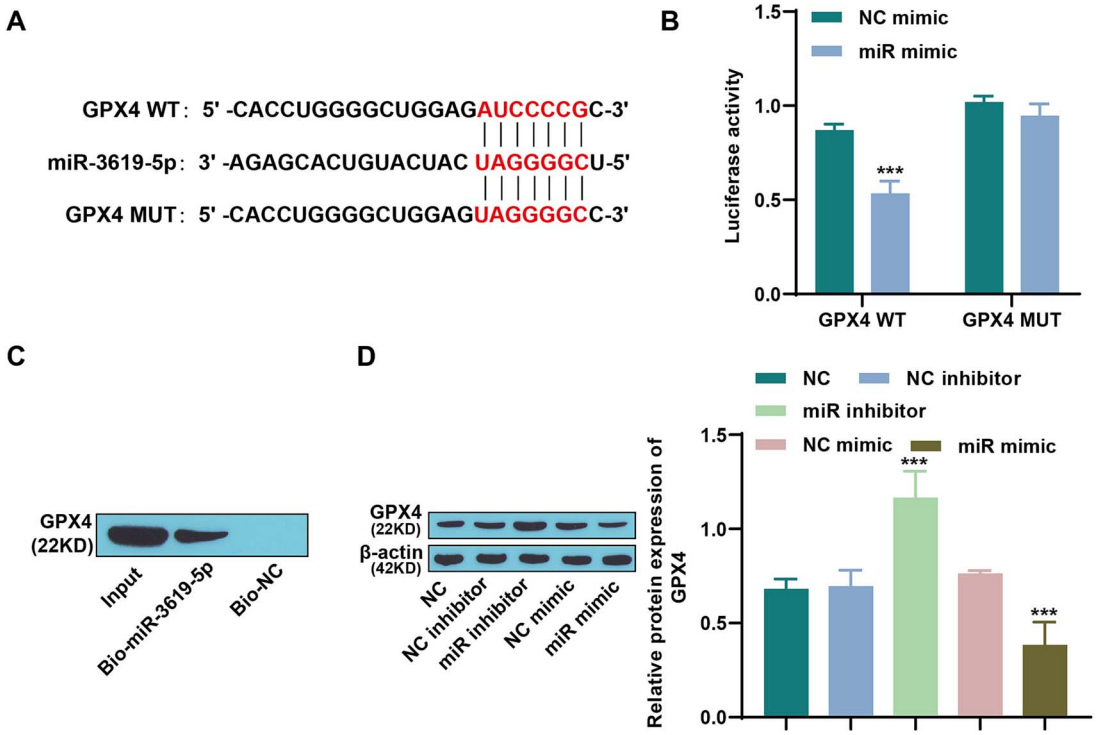

Fig. 5. miR-3,619-5p targets the expression of GPX4. A: TargetScan was used to predict the binding sites between miR-3,619-5p and GPX4. B: The interaction between miR-3,619-5p and GPX4 was verified by a dual-luciferase reporter gene assay. C: RNA pull-down validation of the interaction between miR-3,619-5p and GPX4. D: Western blot analysis of GPX4. ***$P < 0.001$ vs. the NC mimic or NC.

reduced total Fe and Fe^{2+} levels in cells, but treatment with erastin increased the total Fe and Fe^{2+} levels (Fig. 4E and F). Western blot analysis of the expression of ferroptosis-related proteins revealed that knocking down miR-3,619-5p promoted GPX4 and FTH1 expression but inhibited ACSL4 expression; however, treatment with erastin reversed the effect of miR-3,619-5p knockdown (Fig. 4G). Therefore, these findings indicated that miR-3,619-5p is involved in the regulation of CSE-induced ferroptosis in HBE cells.

3.5 Targeted regulation of GPX4 expression by miR-3,619-5p

The specific mechanism by which miR-3,619-5p regulates ferroptosis was subsequently explored. Because GPX4 is a negative regulator of ferroptosis[12,13] and plays a role in protecting against cell damage,[14] the target binding relationship of miR-3,619-5p was predicted using TargetScan (https://www.targetscan.org/vert_80, which predicted that GPX4 was the downstream target of miR-3,619-5p (Fig. 5A). The interaction between miR-3,619-5p and GPX4 was confirmed via a dual-luciferase reporter gene assay and RNA pull-down detection (Fig. 5B and C). Finally, detection of GPX4 expression revealed that miR-3,619-5p knockdown promoted GPX4 expression but that miR-3,619-5p overexpression inhibited GPX4 expression (Fig. 5D). These results indicated that miR-3,619-5p negatively regulates the expression of GPX4.

3.6 GPX4 mediates the promoting effect of miR-3,619-5p on CSE-induced ferroptosis in HBE cells

Next, the present study verified whether the effect of miR-3,619-5p on ferroptosis in HBE cells is mediated by GPX4. First, the knockdown efficiency of GPX4 was detected, which revealed that GPX4 expression in the sh-GPX4–1 and sh-GPX4–2 groups was significantly decreased (Fig. 6A). Because the sh-GPX4–2 group had greater knockdown efficiency, sh-GPX4–2 was selected for subsequent experiments. CSE inhibited GPX4 expression, while miR-3,619-5p knockdown promoted GPX4 expression; further transfection of sh-GPX4 reduced GPX4 expression (Fig. 6B). RT–qPCR analysis revealed that miR-3,619-5p knockdown inhibited miR-3,619-5p expression, whereas further knockdown of GPX4 had no significant effect on miR-3,619-5p (Fig. 6C). The oxidative stress assay revealed that miR-3,619-5p knockdown significantly increased GSH levels, reduced ROS levels, and reduced MDA levels, while further knockdown of GPX4 weakened the effect of the miR-3,619-5p inhibitor (Fig. 6D–F). Iron level detection revealed that miR-3,619-5p knockdown significantly reduced total iron and Fe^{2+} levels, whereas further knockdown of GPX4 significantly increased total iron and Fe^{2+} levels (Fig. 6G and H). These results indicated that the promoting effect of miR-3,619-5p on CSE-induced ferroptosis in HBE cells is achieved by inhibiting GPX4.

3.7 GBE inhibits CS-induced COPD development in mice

To determine whether GBE inhibits the development of COPD in vivo, a mouse model was utilized. Detection of the number of inflammatory cells in the BALF revealed that CS treatment significantly increased the number of macrophages, lymphocytes, and neutrophils, whereas GBE treatment reduced the number of related inflammatory cells (Fig. 7A–D). ELISA detection of inflammatory factors in lung tissue revealed that CS treatment significantly increased the levels of IL-6, IL-8, and TNF-α, whereas GBE treatment decreased the levels of these inflammatory factors (Fig. 7E). In addition, the CS group exhibited alveolar structure destruction, increased infiltration of inflammatory cells, and expanded alveolar spaces. GBE treatment partially restored the

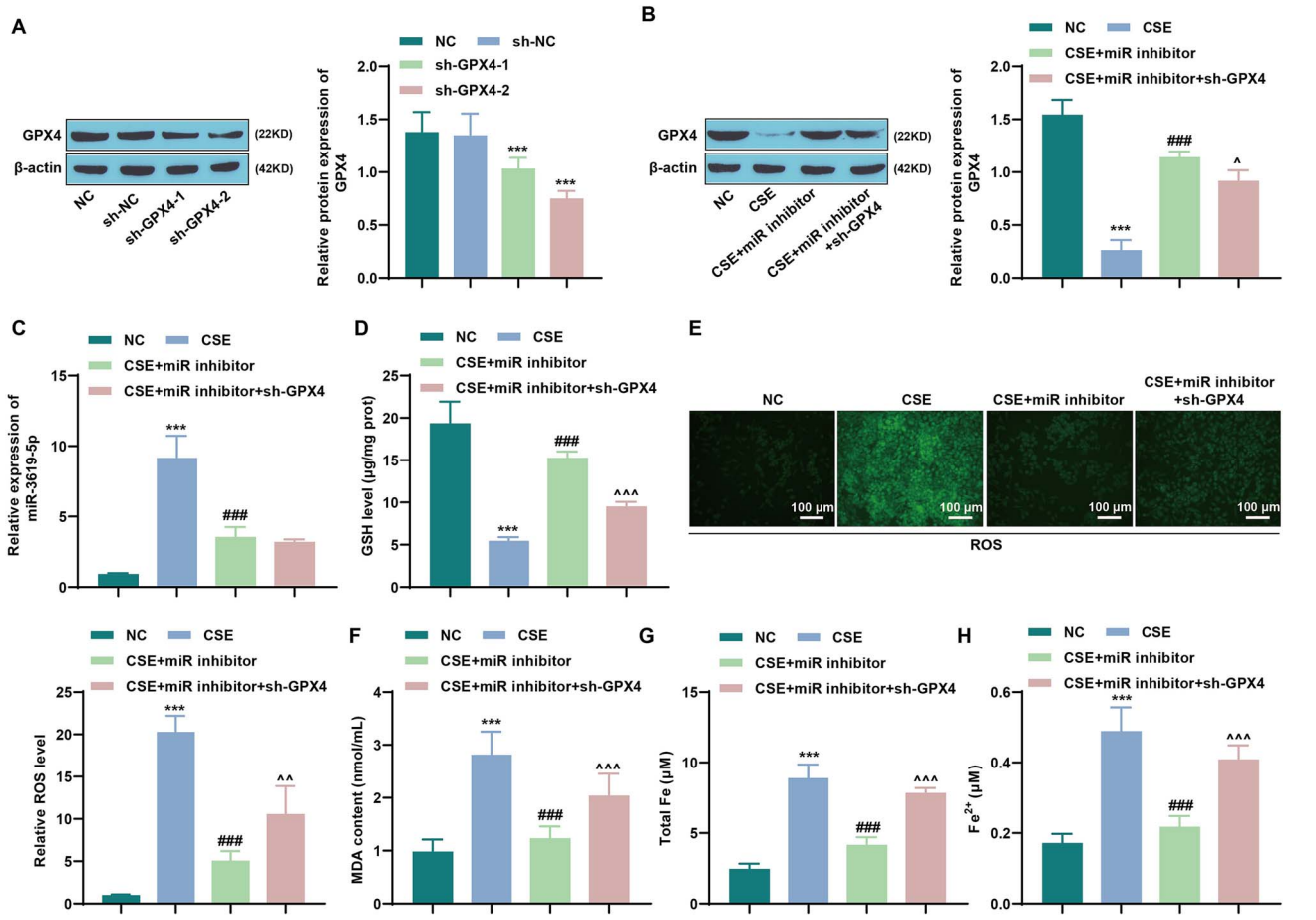

Fig. 6. GPX4 mediates the promoting effect of miR-3,619-5p on CSE-induced ferroptosis in HBE cells. A: Western blot analysis of sh-GPX4 transfection efficiency. B: Western blot analysis of GPX4 expression. C: RT–qPCR detection of miR-3,619-5p levels. D: Detection of GSH levels via a reagent kit. E: Detection of ROS levels via a DCFH–DA fluorescence probe. F: Detection of MDA levels via a reagent kit. G: Testing the total iron level via a reagent kit. H: A reagent kit was used to detect Fe^{2+} levels. $^{***}P < 0.001$ vs. NC; $^{\#\#\#}P < 0.001$ vs. CSE; $^{\wedge}P < 0.05$, $^{\wedge\wedge}P < 0.01$ and $^{\wedge\wedge\wedge}P < 0.001$ vs. CSE + miR inhibitor.,

alveolar structure of the mice and reduced the infiltration of inflammatory cells (Fig. 7F). Western blot analysis of ferroptosis-related protein expression revealed that compared with the control group, CS treatment significantly inhibited the expression of GPX4 and FTH1 but promoted the expression of ACSL4; however, GBE treatment weakened the effect of CS (Fig. 7G). TUNEL staining revealed that CS treatment significantly promoted apoptosis, whereas GBE treatment significantly inhibited apoptosis (Fig. 7H). These results indicated that GBE treatment inhibits the progression of COPD induced by CS in mice.

4 Discussion

COPD is a complex lung disease characterized by emphysema and progressive airflow obstruction. As one of the main pathogenic factors, CS stimulates the production and accumulation of ROS, and it induces lipid peroxidation and ferroptosis in COPD.[16] Understanding the mechanism of ferroptosis in COPD may be valuable for determining drug treatment. The present study utilized an experimental COPD model and demonstrated that GBE inhibits ferroptosis in HBE cells, thereby alleviating COPD progression. These findings suggested that exploring the molecular mechanism by which GBE inhibits ferroptosis in COPD is important.

Ferroptosis is a new type of regulatory cell death that is more immunogenic than cell apoptosis because it involves the release of damage-related molecular patterns and warning factors, as well as the transformation of the extracellular environment into a proinflammatory state.[28,29] Ferroptosis is associated with cancer, degenerative brain disease, ischemia–reperfusion injury, and lung disease.[30–32] Yoshida et al.[16] reported that ferroptosis in COPD triggers cellular damage mechanisms, resulting in the release of ROS and inflammatory factors, ultimately leading to emphysema and airway stenosis in COPD patients. The present study used a CSE-induced cell model and a CS-induced COPD mouse model. In the BALF of COPD mice, the number of inflammatory cells was increased, the alveolar structure was destroyed, and the levels of inflammatory factors in the lung tissue were increased, representing similar pathological features of human COPD.[33] In experimental COPD models, the expression levels of the GPX4 and FTH1 ferroptosis-related proteins were significantly downregulated, and the expression of ACSL4 was significantly upregulated. Moreover, CSE treatment led to deposition of total iron and Fe^{2+} in HBE cells, as well as production of lipid peroxidation products, reduction in cell viability, and release of IL-6, IL-8, and TNF-α. These results suggested that ferroptosis plays an important role in the development of COPD and that inhibiting ferroptosis may be a new target for the treatment of COPD.

G. biloba leaves belong to the lung meridian, and they promote blood circulation, clear collaterals, resolve phlegm, moisten the lungs, and relieve asthma. Shuxuening injection is a sterilized aqueous solution extracted from *G. biloba* leaves. It has been reported that GBE partially or significantly reverses endothelial

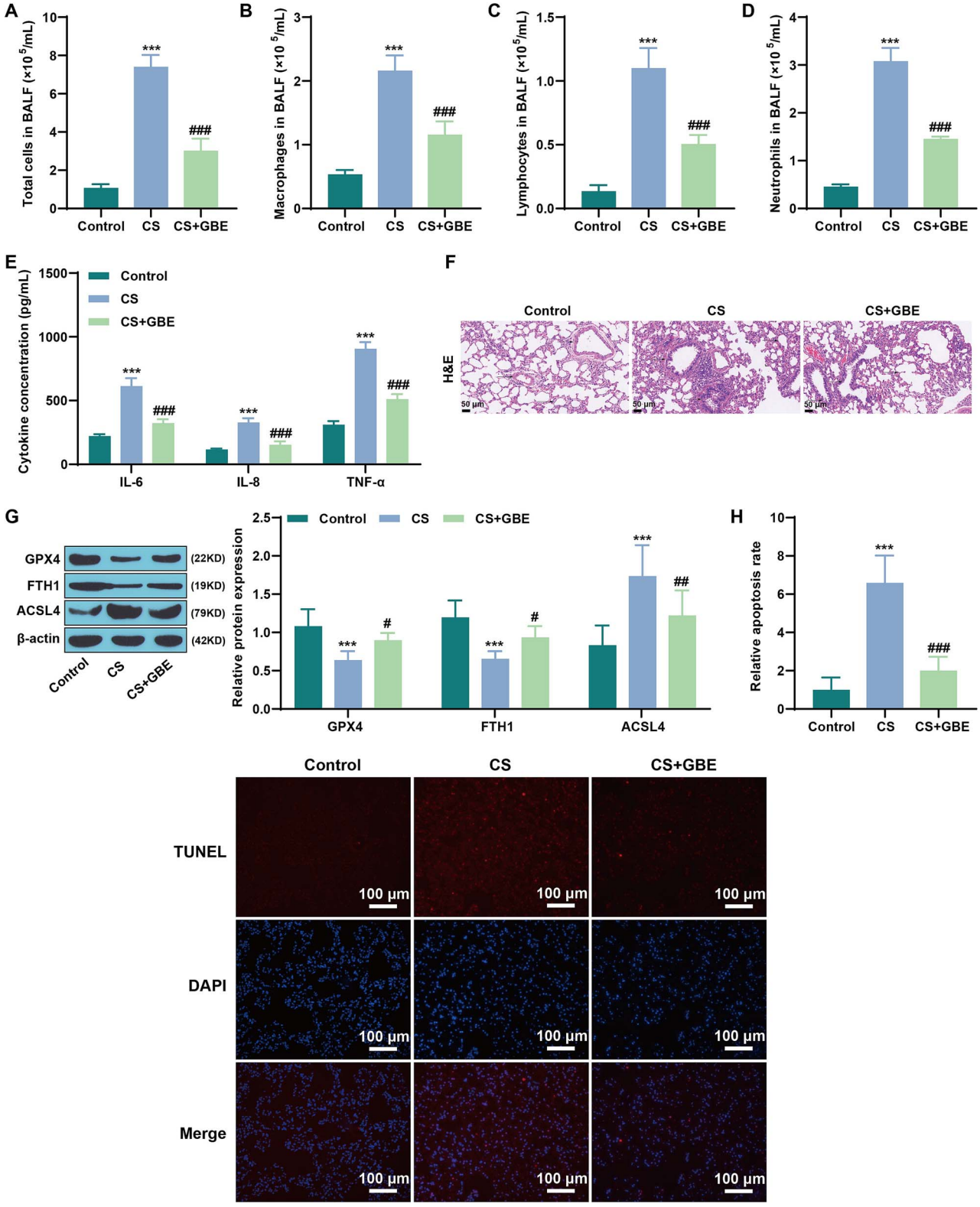

Fig. 7. GBE inhibits CS-induced COPD development in mice. A-D: Cell counts of inflammatory cells (macrophages, lymphocytes, and neutrophils) in the BALF. E: ELISA detection of inflammatory factors. F: HE staining was used to evaluate histopathological changes in the lung tissue. G: Western blot analysis of ferroptosis-related proteins. H: TUNEL staining detection of the degree of apoptosis. $^{***}P < 0.001$ vs. control; $^{\#}P < 0.05$, $^{\#\#}P < 0.01$, and $^{\#\#\#}P < 0.001$ vs. CS.

dysfunction caused by hypoxia,[34] and GBE also exerts antioxidant effects, clears free radicals, reduces blood viscosity, alleviates airway inflammation, and prevents adhesion among platelets, white blood cells, and endothelial cells.[35] In lung-related diseases, Yao et al.[36] showed that GBE alleviates LPS-induced inflammation in acute lung injury by inhibiting the COX-2 and NF-κB pathways.

Hsu et al.[7] reported that GBE protects human pulmonary artery endothelial cells from the effects of CSE. In addition, the recommended human dosage of GBE is not the same for different diseases.[37,38] The present study demonstrated that HBE cell viability increased in a concentration-dependent manner, and 30 μg/mL GBE was selected for the experiments, which may provide a potential theoretical reference for future human studies. The present study also investigated the impact of GBE on the progression of COPD. In both the CSE-induced cell model and the CS-induced animal model, GBE treatment effectively reduced the levels of the IL-6, IL-8, and TNF-α inflammatory factors, as well as the production of ROS and MDA. In addition, GBE treatment promoted the expression of the GPX4 and FTH1 ferroptosis-related proteins but reduced the number of inflammatory cells in the BALF, and it improved cell viability, reduced ferroptosis, and alleviated COPD. These results suggested that GBE may be used to treat COPD by inhibiting ferroptosis.

It is important to determine how GBE regulates ferroptosis to affect the progression of COPD. In recent years, many miRNAs have been shown to be involved in the occurrence of COPD, affecting various aspects of lung injury. Research has shown that miR-212-5p alleviates COPD by inhibiting inflammatory responses and promoting cell proliferation.[39] miR-26a-5p regulates the PTGS2/PGE2 pathway to inhibit ferroptosis, thereby improving airway remodeling in COPD patients.[40] The present study focused mainly on miR-3,619-5p, which has been widely studied in many diseases. For example, Sun et al.[41] showed that miR-3,619-5p inhibits the progression of colorectal cancer, and Ge et al.[42] reported that the miR-3,619-5p overexpression alleviates the progression of non-small cell lung cancer. However, there are currently no reports on the regulation of ferroptosis by miR-3,619-5p. The present study demonstrated that the expression of miR-3,619-5p significantly increased in the COPD cell model, indicating that miR-3,619-5p is involved in the process of HBE cell damage. The increase in miR-3,619-5p expression may be one of the factors contributing to COPD. GBE treatment significantly reduced the expression level of miR-3,619-5p, whereas miR-3,619-5p overexpression reversed the effects of GBE treatment, significantly promoting the release of the IL-6, IL-8, and TNF-α inflammatory factors, as well as the production of ROS and MDA; in addition, miR-3,619-5p overexpression inhibited the expression of the GPX4 and FTH1 ferroptosis-related proteins, thereby promoting ferroptosis. These findings indicated that GBE regulates the ferroptosis process of HBE cells through miR-3,619-5p.

In addition, the present study showed that miR-3,619-5p targeted and inhibited GPX4, which may be an important mechanism by which miR-3,619-5p regulates ferroptosis in HBE cells. GPX4 reduces iron-dependent ROS formation by regulating GSH expression[43,44] and this process is inhibited by a GPX4 inhibitor, such as ML162.[44] In the present study, CSE inhibited GPX4 expression, and miR-3,619-5p knockdown promoted GPX4 expression, inhibited ROS production, inhibited MDA production, increased GSH levels, and reduced total iron and Fe^{2+} levels, thereby inhibiting the ferroptosis process in HBE cells. However, GPX4 knockdown weakened the protective effect of miR-3,619-5p knockdown on HBE cells. These results indicated that miR-3,619-5p knockdown inhibits CSE-induced ferroptosis in HBE cells by promoting GPX4 expression.

However, the present study had some limitations. GBE contains various active constituents, including ginkgolide A, ginkgolide B, ginkgolide C, ginkgolide J, bilobalide, and quercetin, etc.[45] Ginkgolide B, the active constituent of GBE, inhibits the ubiquitination of GPX4 in MPC5 cells to inhibit ferroptosis.[18] Therefore, more detailed studies are needed in the future to distinguish the mechanism of action of individual constituents of GBE on ferroptosis in COPD to better understand the effectiveness and complexity of GBE in COPD patients. In addition, because COPD is associated with inhalation exposure, the use of an air–liquid interface (ALI) culture system to culture HBE cells should be considered in future experimental designs to better simulate the in vivo environment.

In summary, the present study revealed that GBE treatment promotes GPX4 expression by inhibiting miR-3,619-5p, thereby blocking CSE-induced pulmonary epithelial cell ferroptosis and alleviating the progression of COPD. The present results suggest that GBE may be an effective therapeutic drug for COPD and that targeting the miR-3,619-5p/GPX4 molecular axis may provide a new therapeutic strategy for preventing COPD.

Acknowledgments

Not applicable.

Author contributions

Anhui Xu, Yanmei Xu, and Hongbo Chen wrote the main manuscript; Anhui Xu prepared Figs 1–3; Yanmei Xu prepared Figs 4,5; Hongbo Chen prepared Figs 6–7; Linhua Xiang prepared the attached figures; and Xiao Zhao revised the manuscript. All the authors have read and approved the final manuscript.

Supplementary material

Supplementary material is available at *TOXRES Journal* online.

Funding

Not applicable.

Conflicts of interest: The authors declare that they have no competing interests.

Data availability

All the methods/studies were conducted in accordance with the Declaration of Helsinki, and all the animal experiments were conducted in accordance with the ARRIVE guidelines.

Availability of data and materials

The datasets used and/or analyzed during the current study are available from the corresponding author upon reasonable request.

References

1. Brillet PY et al. Investigation of airways using MDCT for visual and quantitative assessment in COPD patients. *Int J Chron Obstruct Pulm Dis*. 2008:3:97–107. https://doi.org/10.2147/copd.s2302
2. Zhang Z et al. Hypermethylation of the Nrf2 promoter induces Ferroptosis by inhibiting the Nrf2-GPX4 Axis in COPD. *Int J Chron Obstruct Pulm Dis*. 2021:16:3347–3362.

3. Higashi T et al. A simple and rapid method for standard preparation of gas phase extract of cigarette smoke. *PLoS One*. 2014:9:e107856. https://doi.org/10.1371/journal.pone.0107856
4. Linkermann A, Stockwell BR, Krautwald S, Anders HJ. Regulated cell death and inflammation: an auto-amplification loop causes organ failure. *Nat Rev Immunol*. 2014:14:759–767. https://doi.org/10.1038/nri3743
5. Tao Z et al. Evaluation of the anti-inflammatory properties of the active constituents in Ginkgo biloba for the treatment of pulmonary diseases. *Food Funct*. 2019:10:2209–2220. https://doi.org/10.1039/C8FO02506A
6. Diamond BJ, Bailey MR. Ginkgo biloba: indications, mechanisms, and safety. *Psychiatr clin North Am*. 2013:36:73–83. https://doi.org/10.1016/j.psc.2012.12.006
7. Hsu CL, Wu YL, Tang GJ, Lee TS, Kou YR. Ginkgo biloba extract confers protection from cigarette smoke extract-induced apoptosis in human lung endothelial cells: role of heme oxygenase-1. *Pulm Pharmacol Ther*. 2009:22:286–296. https://doi.org/10.1016/j.pupt.2009.02.003
8. Tang Y et al. The effect of ginkgo Biloba extract on the expression of PKCα in the inflammatory cells and the level of IL-5 in induced sputum of asthmatic patients. *J Huazhong Univ Sci Technolog Med Sci*. 2007:27:375–380.
9. Pan L et al. Ginkgo biloba extract EGb761 attenuates Bleomycin-induced experimental pulmonary fibrosis in mice by regulating the balance of M1/M2 macrophages and nuclear factor kappa B (NF-κB)-mediated cellular apoptosis. *Med sci Monit: Int Med J Exp Clin Res*. 2020:26:e922634. https://doi.org/10.12659/MSM.922634
10. Lee CY et al. Protective effect of Ginkgo biloba leaves extract, EGb761, on endotoxin-induced acute lung injury via a JNK- and Akt-dependent NFκB pathway. *J Agric Food Chem*. 2014:62:6337–6344. https://doi.org/10.1021/jf501913b
11. Li Y, Yang Y, Yang Y. Multifaceted roles of Ferroptosis in lung diseases. *Front Mol Biosci*. 2022:9:919187.
12. Friedmann Angeli JP et al. Inactivation of the ferroptosis regulator Gpx4 triggers acute renal failure in mice. *Nat Cell Biol*. 2014:16:1180–1191. https://doi.org/10.1038/ncb3064
13. Imai H et al. Early embryonic lethality caused by targeted disruption of the mouse PHGPx gene. *Biochem Biophys Res Commun*. 2003:305:278–286. https://doi.org/10.1016/S0006-291X(03)00734-4
14. Stoyanovsky DA et al. Iron catalysis of lipid peroxidation in ferroptosis: regulated enzymatic or random free radical reaction? *Free Radic Biol Med*. 2019:133:153–161. https://doi.org/10.1016/j.freeradbiomed.2018.09.008
15. Yu S et al. Recent progress of Ferroptosis in lung diseases. *Front Cell Dev Biol*. 2021:9:789517.
16. Yoshida M et al. Involvement of cigarette smoke-induced epithelial cell ferroptosis in COPD pathogenesis. *Nat Commun*. 2019:10:3145.
17. Tao Z et al. Therapeutic effect of ginkgetin on smoke-induced airway inflammation by down-regulating the c/EBPβ signaling pathway and CCL2 expression. *J Ethnopharmacol*. 2024:331:118284. https://doi.org/10.1016/j.jep.2024.118284
18. Chen J et al. Ginkgolide B alleviates oxidative stress and ferroptosis by inhibiting GPX4 ubiquitination to improve diabetic nephropathy. *Biomed Pharmacother*. 2022:156:113953. https://doi.org/10.1016/j.biopha.2022.113953
19. Ding C et al. miR-182-5p and miR-378a-3p regulate ferroptosis in I/R-induced renal injury. *Cell Death Dis*. 2020:11:929.
20. Zhang H et al. CAF secreted miR-522 suppresses ferroptosis and promotes acquired chemo-resistance in gastric cancer. *Mol Cancer*. 2020:19:43.
21. Gómez-Cabello D et al. DGCR8-mediated disruption of miRNA biogenesis induces cellular senescence in primary fibroblasts. *Aging Cell*. 2013:12:923–931. https://doi.org/10.1111/acel.12117
22. Lu TX, Rothenberg ME. MicroRNA. *J Allergy Clin Immunol*. 2018:141:1202–1207. https://doi.org/10.1016/j.jaci.2017.08.034
23. Sundar IK, Li D, Rahman I. Small RNA-sequence analysis of plasma-derived extracellular vesicle miRNAs in smokers and patients with chronic obstructive pulmonary disease as circulating biomarkers. *J Extracell Vesicles*. 2019:8:1684816.
24. Niu X, Liu S, Jia L, Chen J. Role of MiR-3619-5p in β-catenin-mediated non-small cell lung cancer growth and invasion. *Cell Physiol Biochem*. 2015:37:1527–1536. https://doi.org/10.1159/000438520
25. Xia H et al. Long noncoding HOXA11-AS knockdown suppresses the progression of non-small cell lung cancer by regulating miR-3619-5p/SALL4 axis. *J Mol Histol*. 2021:52:729–740. https://doi.org/10.1007/s10735-021-09981-1
26. Zhou H et al. CD147 promoted epithelial mesenchymal transition in airway epithelial cells induced by cigarette smoke via oxidative stress Signaling pathway. *Copd*. 2020:17:269–279. https://doi.org/10.1080/15412555.2020.1758051
27. Fujii S et al. Insufficient autophagy promotes bronchial epithelial cell senescence in chronic obstructive pulmonary disease. *Onco Targets Ther*. 2012:1:630–641. https://doi.org/10.4161/onci.20297
28. Sun Y et al. The emerging role of ferroptosis in inflammation. *Biomed pharmacother*. 2020:127:110108. https://doi.org/10.1016/j.biopha.2020.110108
29. Yang WS, Sriramaratnam R, Welsch ME, et al. Regulation of ferroptotic cancer cell death by GPX4. *Cell*. 2014:156:317–331. https://doi.org/10.1016/j.cell.2013.12.010
30. Shin D, Kim EH, Lee J, Roh JL. Nrf2 inhibition reverses resistance to GPX4 inhibitor-induced ferroptosis in head and neck cancer. *Free Radic Biol Med*. 2018:129:454–462. https://doi.org/10.1016/j.freeradbiomed.2018.10.426
31. Ma H et al. Melatonin suppresses Ferroptosis induced by high glucose via activation of the Nrf2/HO-1 Signaling pathway in type 2 diabetic osteoporosis. *Oxidative Med Cell Longev*. 2020:2020:1–18.
32. Liu P et al. Ferrostatin-1 alleviates lipopolysaccharide-induced acute lung injury via inhibiting ferroptosis. *Cell Mol Biol Lett*. 2020:25:10.
33. Guo P et al. Pathological mechanism and targeted drugs of COPD. *Int J Chron Obstruct Pulmon Dis*. 2022:Volume 17:1565–1575. https://doi.org/10.2147/COPD.S366126
34. Shen JY, Sun AJ, Gu XM. Effects of Ginkgo biloba extract 50 on hypoxia induced endothelial dysfunction. *Zhongguo Zhong Xi Yi Jie He Za Zhi*. 2007:27:151–154.
35. Huang CH et al. Ginkgo biloba leaves extract (EGb 761) attenuates lipopolysaccharide-induced acute lung injury via inhibition of oxidative stress and NF-κB-dependent matrix metalloproteinase-9 pathway. *Phytomedicine*. 2013:20:303–309. https://doi.org/10.1016/j.phymed.2012.11.004
36. Yao X, Chen N, Ma CH, et al. Ginkgo biloba extracts attenuate lipopolysaccharide-induced inflammatory responses in acute lung injury by inhibiting the COX-2 and NF-κB pathways. *Chin J Nat Med*. 2015:13:52–58. https://doi.org/10.1016/S1875-5364(15)60006-1
37. Labkovich M, Jacobs EB, Bhargava S, Pasquale LR, Ritch R. Ginkgo Biloba extract in ophthalmic and systemic disease, with a focus on normal-tension glaucoma. *Asia Pac J Ophthalmol (Phila)*. 2020:9:215–225.

38. Evans JR. Ginkgo biloba extract for age-related macular degeneration. *Cochrane Database Syst Rev*. 2013:2013:Cd001775.
39. Jia Q et al. MiR-212-5p exerts a protective effect in chronic obstructive pulmonary disease. *Discov Med*. 2018:26:173–183.
40. Liu C, Lu J, Yuan T, Xie L, Zhang L. EPC-exosomal miR-26a-5p improves airway remodeling in COPD by inhibiting ferroptosis of bronchial epithelial cells via PTGS2/PGE2 signaling pathway. *Sci Rep*. 2023:13:6126.
41. Sun Y et al. Downregulation of LINC00958 inhibits proliferation, invasion and migration, and promotes apoptosis of colorectal cancer cells by targeting miR-3619-5p. *Oncol Rep*. 2020:44:1574–1582. https://doi.org/10.3892/or.2020.7707
42. Ge L, Tan W, Li G, Gong N, Zhou L. Circ_0026134 promotes NSCLC progression by the miR-3619-5p/CHAF1B axis. *Thorac Cancer*. 2022:13:582–592. https://doi.org/10.1111/1759-7714.14301
43. Tang H et al. Dual GSH-exhausting sorafenib loaded manganese-silica nanodrugs for inducing the ferroptosis of hepatocellular carcinoma cells. *Int J Pharm*. 2019:572:118782. https://doi.org/10.1016/j.ijpharm.2019.118782
44. Forcina GC, Dixon SJ. GPX4 at the crossroads of lipid homeostasis and Ferroptosis. *Proteomics*. 2019:19:e1800311. https://doi.org/10.1002/pmic.201800311
45. Singh SK, Srivastav S, Castellani RJ, Plascencia-Villa G, Perry G. Neuroprotective and antioxidant effect of Ginkgo biloba extract against AD and other neurological disorders. *Neurotherapeutics*. 2019:16:666–674. https://doi.org/10.1007/s13311-019-00767-8

Toxicology Research, 2025, **14**, 1–12
https://doi.org/10.1093/toxres/tfae225
Paper